GEOPHYSICS, VOL. 46, NO. 3 (MARCH 1981); P. 309–315, 4 FIGS.

# Electromagnetic field of a dipole on a two-layer earth

W. C. Chew* and J. A. Kong*


## ABSTRACT

The electromagnetic field due to a horizontal electric dipole placed on top of a two-layer earth is represented in terms of fields due to a dipole over a half-space earth and its image source fields. Integral representations of image source fields are evaluated with uniform asymptotic approximations. Leading order ordinary saddle-point approximation, giving rise to the geometrical optics approximation (GOA), is shown to be inaccurate. This is especially true when the angle of observation is close to the critical angle, which corresponds to the presence of a branch-point singularity near the saddle point. In the uniform asymptotic approximation, the integrand of the image source integral is split into a branch-point free part and another part containing the branch-point singularity. The branch-point free part can be approximated with a spherical wave function, while the part containing the branch point can be approximated with parabolic cylinder functions. Vertical magnetic field components and the horizontal electric field component near the surface are illustrated and compared with the geometrical optics approximation, giving the direct numerical result as well as experimental measurement. It is shown that the uniform asymptotic approximation yields excellent agreement with numerical and experimental results compared to the geometrical optics approximation.


## INTRODUCTION

The electromagnetic (EM) field of a dipole antenna over a layered medium has been a subject of continued interest due to its application in geophysical subsurface probing (Wait, 1951, 1970, 1971; Brekhovskikh, 1960; Kong et al, 1972, 1974, 1975, 1977; Tsang et al, 1973, 1974; Felsen and Marcuvitz, 1973; Annan, 1973, 1975; Rossiter et al, 1973, 1975). Analytical approximations for the interference field have been obtained using the normal-mode expansion method and the geometrical optics approximation (GOA) (Annan, 1973, 1975; Tsang and Kong, 1973; Kong et al, 1974; Rossiter et al, 1973, 1975). In the normal-mode expansion method, the field in the layered medium is decomposed into guided modes. It is an efficient method only if the layer thickness is much smaller than the wavelength such that the number of guided modes that need to be considered is small. In GOA, the interference field is expressed as a superposition of fields from the dipole source and its image sources. Fields from the image sources are represented as rays undergoing multiple reflections within the layered medium. The GOA can be verified from the integral representations of the image source fields by using the ordinary saddle-point approximation. It is found that GOA is good when layer thicknesses are large compared to wavelength, i.e., in the domain where geometrical optics applies.

However, there are limitations in GOA, for when the point of observation is not far from the image sources, the ordinary saddle-point approximation deteriorates, especially when the observation point is in the caustics of geometrical optics. Mathematically, this is due to the proximity of a branch point to the saddle point which modifies the field due to an image source when the angle of observation is close to the critical angle.

We investigate the $H_z$ and $E_\phi$ components of the field due to a horizontal electric dipole on a two-layer earth. We shall approximate the integral representation of the image source field using a uniform asymptotic expansion method (Bleistein and Handelsman, 1975) which is uniformly valid for all angles of observation. For the case where the image source and observation-point separation is large, and the angle of observation-point separation is not close to the critical angle, we can show that the uniform asymptotic approximation (UAA) reduces to that of geometrical optics approximation. An important reason for using UAA is that we can extend the range for which the approximation of the image-source representation of the field is valid into the domain where the modal representation of the field has been superior before (Annan, 1973; Kong, 1974). Use of the normal-mode expansion method involves numerical search for poles on the complex plane, which becomes inefficient for thick layers. In comparison, the image source representation of the field with UAA is demonstrably a more efficient method to use, complementing the normal mode approach for thin layers.

## FORMULATION

With the image-source representation, field components $H_z$ and $E_\phi$ in the upper half-space due to a horizontal electric dipole antenna over a two-layer medium (Figure 1) take the following form (Tsang and Kong, 1973),

$$H_z = -i\frac{Il}{8\pi}\frac{\partial}{\partial\rho}T\sin\phi, \tag{1a}$$

Manuscript received by the Editor October 18, 1979; revised manuscript received June 30, 1980.
*Department of Electrical Engineering, Computer Science and Research Laboratory of Electronics, Massachusetts Institute of Technology, Cambridge, MA 02139.

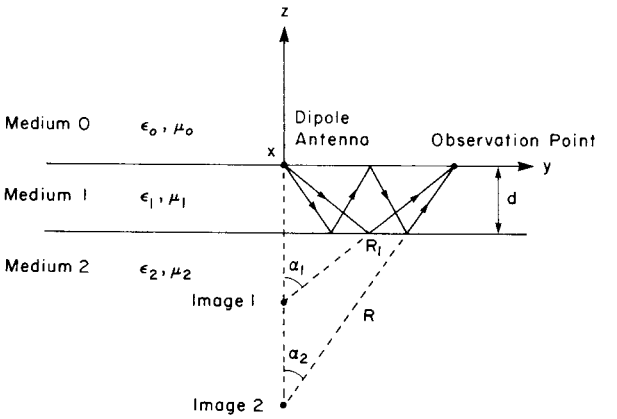


FIG. 1. A dipole antenna on a two-layer medium.

$$E_\phi \simeq \frac{\omega\mu Il}{8\pi} T_v \sin\phi \tag{1b}$$

with

$$T = \int_{-\infty}^{\infty} \frac{k_\rho}{k_z} X_{01} H_0^{(1)}(k_\rho\rho) e^{ik_z z} dk_\rho + \sum_{m=1}^{\infty} \int_{-\infty}^{\infty} \frac{k_\rho}{k_z} X_{01} X_{10} R_{10}^{m-1} R_{12}^m e^{ik_z z} e^{ik_{1z} 2md} H_0^{(1)}(k_\rho\rho) dk_\rho \tag{2}$$

where

$$R_{ij} = \frac{k_{iz} - \frac{\mu_i}{\mu_j} k_{jz}}{k_{iz} + \frac{\mu_i}{\mu_j} k_{jz}},$$

$X_{ij} = 1 + R_{ij}$ are the Fresnel reflection coefficient and transmission coefficient, respectively, for a wave incident from the $i$th medium to the $j$th medium. We have used the time-dependent factor $\exp(-i\omega t)$. Note that expression (2) is valid only in region 0. The dispersion relation for the $i$th medium states that $k_i^2 = k_\rho^2 + k_{iz}^2 = \omega^2 \mu_i \varepsilon_i$ and we ignore subscript 0 for medium 0. The integration path in expression (2) is taken to be the Sommerfeld integration path, which is above the real axis when $k_\rho \leq 0$ passes above the origin, and is below the real axis when $k_\rho > 0$.

Physically the first term of expression (2) gives rise to the half-space solution in the absence of the subsurface layer. The second term, which is a summation of series, corresponds to waves which have reached the surface through multiple reflections from the subsurface. It can also be interpreted as fields due to the image sources of the dipole at $z = -2md$, $m = 1, 2, \ldots$.

A typical image-source term in expression (2) is

$$T_m = \int_{-\infty}^{\infty} \frac{k_\rho}{k_{1z}} A_m(k_\rho)\, e^{ik_{1z}2md} H_0^{(1)}(k_\rho\rho) dk_\rho, \tag{3a}$$

where

$$A_m(k_\rho) = \frac{k_{1z}}{k_z} X_{01} X_{10} R_{10}^{m-1} R_{12}^m e^{ik_z z}. \tag{3b}$$

The above integral has been evaluated (Tsang and Kong, 1973) with the saddle-point method to leading order giving

$$T_m \sim \frac{2e^{ik_1 R_m}}{iR_m} \frac{k_1 \cos\alpha_m}{\sqrt{k^2 - k_1^2 \sin^2\alpha_m}} \cdot X_{01} R_{12}^m R_{10}^{m-1} X_{10} \exp(i\sqrt{k^2 - k_1^2 \sin^2\alpha_m}\, z). \tag{4}$$

where $R_m = [\rho^2 + (2md)^2]^{1/2}$ and $\alpha_m = \tan^{-1}(\rho/2md)$ as shown in Figure 1. Equation (4) states that the spherical wave is multiply reflected and transmitted as in the geometrical optics theory. The factor preceding the transmission and reflection coefficients is imperative for energy conservation.

To improve the GOA, we factor out the $k_z$-dependence in $A_m(k_\rho)$, corresponding to the branch point due to $k_z = \sqrt{k^2 - k_\rho^2}$ at $k_\rho = k$, which can be close to the saddle point. To do this, we first multiply the numerators and the denominators of $X_{10}$ and $R_{10}$ by $k_{1z} - b k_z$, where $b = \mu_1/\mu$. Now the denominators of $X_{10}$ and $R_{10}$ are functions of $k_{1z}^2 - b^2 k_z^2$, which is normal. We then expand the numerator using binomial expansion, multiplying out the series. Separating terms with even and odd powers of $k_z$, we obtain for $k_z z \ll 1$

$$A_{m-\text{even}} = \frac{4b R_{12}^m}{[1 - (bk_z/k_{1z})^2]^{m+1}} \sum_{n=0}^{\infty} k_z^{2n} \sum_{r=0}^{\min(2n, 2m)} \binom{2m}{r} \left(\frac{-b}{k_{1z}}\right)^r \frac{(iz)^{2n-r}}{(2n-r)!}, \tag{5a}$$

and

$$A_{m-\text{odd}} = \frac{4b R_{12}^m}{[1 - (bk_z/k_{1z})^2]^{m+1}} k_z \sum_{n=0}^{\infty} k_z^{2n} \sum_{r=0}^{\min(2n+1, 2m)} \binom{2m}{r} \left(\frac{-b}{k_{1z}}\right)^r \frac{(iz)^{2n+1-r}}{(2n+1-r)!}. \tag{5b}$$

We see that only $A_{m-\text{odd}}$ has a branch point at $k_\rho = k$. Therefore, ordinary saddle-point analysis can be applied to the branch-point free $A_{m-\text{even}}$ term. For the $A_{m-\text{odd}}$ term, we rewrite it as

$$A_{m-\text{odd}} = k_z A_{m0}.$$

Letting $\hat{H}_0^{(1)}(k_\rho\rho) = H_0^{(1)}(k_\rho\rho) e^{-ik_\rho\rho}$, we find the $m$th image-source term due to odd powers of $k_z$ is

$$T_m^0 = \int_{-\infty}^{\infty} k_z A_{m0} \frac{k_\rho}{k_{1z}} \hat{H}_0^{(1)}(k_\rho\rho) \exp[iR_m(k_\rho \sin\alpha_m + k_{1z}\cos\alpha_m)] dk_\rho. \tag{6}$$

We find that there is a saddle point at $k_{\rho s} = k_1 \sin\alpha_m$ by differentiating the exponent with respect to $k_\rho$ and setting it equal to zero. The branch point at $k_\rho = k$ can be arbitrarily close to the saddle point when $\alpha_m \simeq \theta_c = \sin^{-1}(k/k_1)$, i.e., near the critical angle $\theta_c$. Letting $\lambda = R_m$, $t = k_\rho - k_1 \sin\alpha_m$, and $t_b = k - k_1 \sin\alpha_m$;

$$f(t) = -i[k_\rho \sin\alpha_m + (k_1^2 - k_\rho^2)^{1/2} \cos\alpha_m],$$

and

$$g(t) = e^{i(\pi/2)}(k + k_\rho)^{1/2} A_{m0} \frac{k_\rho}{k_{1z}} \hat{H}_0^{(1)}(k_\rho\rho); \tag{7}$$

we find that equation (6) becomes

$$T_m^0 = \int_{-\infty}^{\infty} (t - t_b)^{1/2} g(t) e^{-\lambda f(t)} dt. \tag{8}$$

In the next section we shall obtain the UAA to the above integral which is valid for all $t_b$, including the case when the angle of observation is close to the critical angle.

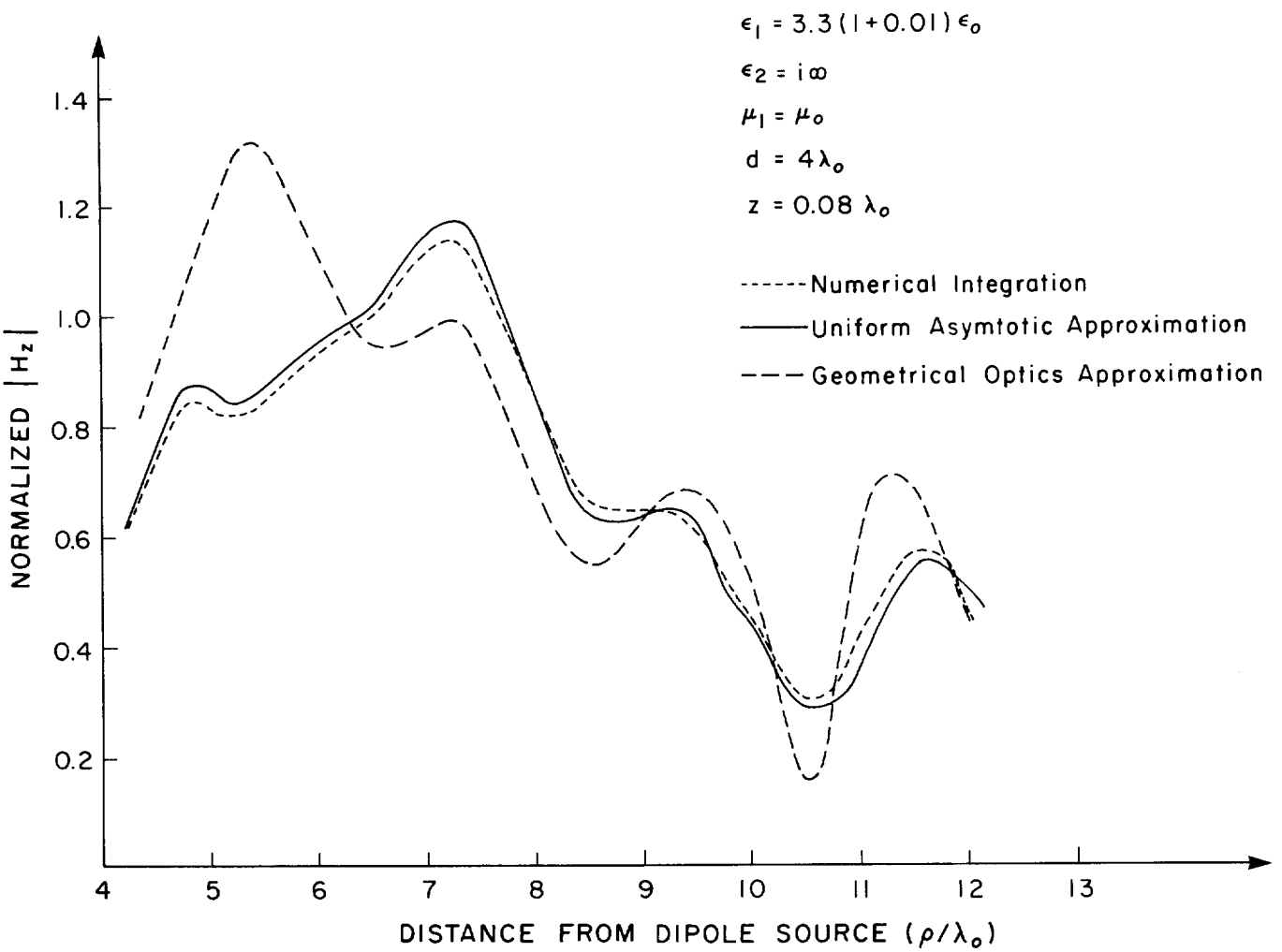


FIG. 2. Normalized $H_z$ component of a horizontal electric dipole in its broadside direction computed from three different approaches ($\lambda_0$ is the free-space wavelength).

## UNIFORM ASYMPTOTIC APPROXIMATION

UAA of the integral in equation (8) can be obtained using Bleistein and Handelsman's (1975) approach described in the Appendix. Making use of the result in the Appendix, we obtain an approximation for equation (6) as:

$$T_m^0 \sim \exp\{ik_1R_m - ik_1R_m \sin^2[(\theta_c - \alpha_m)/2]\} \cdot$$
$$\cdot \sqrt{2\pi}\left\{\frac{G(S_b)}{(2R_m)^{3/4}}\ e^{-i(\pi/4)}D_{1/2}\cdot\right.$$
$$\cdot \left[e^{-i(\pi/4)}2\sqrt{k_1R_m}\sin\left(\frac{\theta_c-\alpha_m}{2}\right)\right]$$
$$+\frac{G(S_b)-G(0)}{S_b(2R_m)^{5/4}}e^{-i(3\pi/4)}D_{3/2}\left[e^{-i(\pi/4)}2\sqrt{k_1R_m}\cdot\right.$$
$$\left.\left.\cdot\sin\left(\frac{\theta_c-\alpha_m}{2}\right)\right]\right\} \qquad (9a)$$

plus higher-order terms, for $R_m \to \infty$, where

$$G(S_b) = e^{i(\pi/8)}\left[\frac{\sqrt{2k_1}\cos\theta_c}{\cos\left(\frac{\theta_c-\alpha_m}{2}\right)}\right]^{3/2}\cdot$$
$$\cdot (2k)^{1/2}A_{m0}(k)\tan\theta_c\,\hat{H}_0^{(1)}(kR_m\sin\alpha_m) \qquad (9b)$$

$$G(0) = e^{i(\pi/8)}\left[(2k_1)^{3/2}\cos\left(\frac{\theta_c+\alpha_m}{2}\right)\right]^{1/2}\cdot$$
$$\cdot \sin\alpha_m(k+k_1\sin\alpha_m)^{1/2}$$
$$A_{m0}(k_1\sin\alpha_m)\,\hat{H}_0^{(1)}(k_1R_m\sin^2\alpha_m) \qquad (9c)$$

and

$$S_b = e^{i(\pi/4)}\sqrt{2k_1}\sin\left(\frac{\theta_c-\alpha_m}{2}\right). \qquad (9d)$$

We arrived at equations (9b) and (9c) by using the fact that

$$\left.\frac{dt}{ds}\right|_{s=0} = e^{-i(\pi/4)}\sqrt{2k_1}\cos\alpha_m \qquad (9e)$$

and

$$\left.\frac{dt}{ds}\right|_{s=s_b} = e^{-i(\pi/4)}\sqrt{2k_1}\,\frac{\cos\theta_c}{\cos\left(\frac{\theta_c-\alpha_m}{2}\right)}. \qquad (9f)$$

We chose the proper branch of square roots in equations (9d), (9e), and (9f) to ensure proper transformation from the $t$-plane to the $s$-plane.

The ordinary saddle-point method can be used to approximate the part of the integral involving $A_{m-\text{even}}$ giving

$$T^e_{im} \sim \frac{2\,e^{ik_1R_m}}{iR_m} A_{m-\text{even}}(k_1 \sin\alpha_m), \qquad (10)$$

which is a spherical wave approximation. As such, we have an asymptotic approximation to $T_{im}$ which is uniformly valid for all angles of observation. The approximation of the first term in equation (2), viz, the half-space solution, can also be obtained using the ordinary saddle-point method. Hence, the asymptotic approximation to equation (2) can be used to find $H_z$ in equation (1).

## RESULTS AND DISCUSSIONS

Using the uniform asymptotic approximation to $H_z$, we obtain a plot of $|H_z|$ versus the distance from the dipole $\rho$ as shown in Figure 2 (taking the first layer to be glacial ice). We also compare our asymptotic approximation with numerical integration of the integral and the GOA. We note excellent agreement of the asymptotic approximation with numerical integration. There are large discrepancies with the GOA, since at one given location $\rho$, one of the observation angles $\alpha_m$ could be close to the critical angle, or the caustics of geometrical optics (Brekhovskikh, 1960). Thus the result from GOA deteriorates.

In Figure 3, we plot $|E_\phi|$ as a function of $\rho$ using UAA and GOA, and compare with experimental measurement using a scaled model tank (Rossiter et al, 1973). The dielectric layer is low loss in this case. We note the excellent agreement of UAA with experimental results when $d = 5\ \lambda_0$. GOA, as noted also in Figure 2, shows an erroneous peak in the field due to the image source when the receiver is located at a point which lies in the caustics of the image

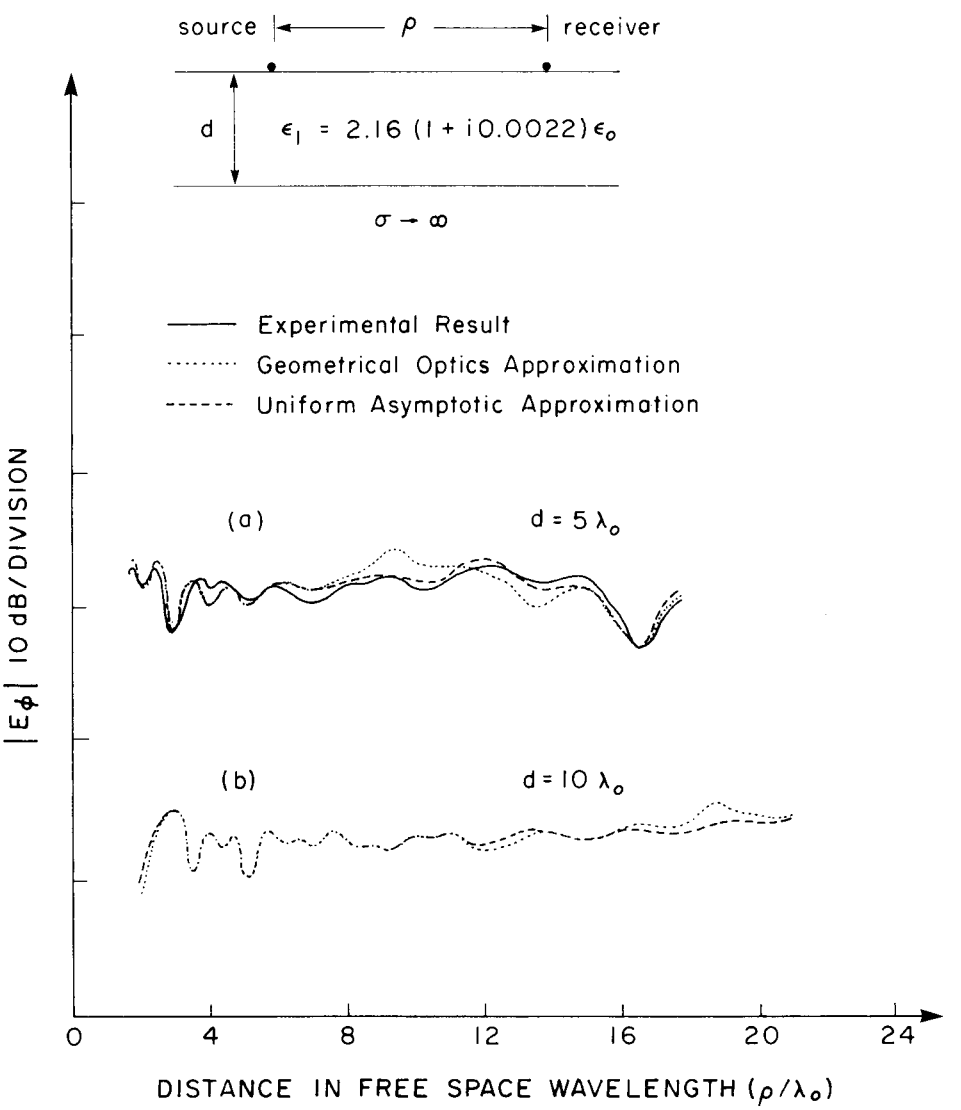


FIG. 3. Comparison of $E_\phi$ component using UAA with GOA and scaled model tank experiment.

field (i.e., at $\rho \simeq k/\sqrt{k_1^2 - k^2}$, which is $\simeq 5.6\ \lambda_0$ in Figure 2 and $\simeq 9.6\ \lambda_0$ in Figure 3). When $d = 10\ \lambda_0$ (Figure 3b), we note that UAA and GOA are in good agreement except when the receiver is at the caustics of the image field.

In Figure 4, we compare the plot of $|H_z|$ with experimental data collected on measurements performed on the Athabasca glacier (Savage and Paterson, 1963). In this case, both the GOA and UAA agree well with the experimental result, even though $d = 1.2\ \lambda$. This is because of the lossy nature of the ice layer. For the $k_1$ complex, the location of the saddle point at $k_1 \sin \alpha_m$ can never coalesce exactly with the branch point at $k$. Furthermore, the contribution of the field due to the image sources diminishes in such a lossy layer.

Consequently, we conclude that for a low-loss medium when the image-source fields are important, the application of UAA as opposed to GOA improves approximation to the image fields, thus extending the range of validity of image-field representation. Previously, the use of GOA to the image field deteriorates, when the receiver is at the caustics of the image field even when the layered earth is very thick (Figure 3b). However, when the layered earth is lossy, GOA and UAA are in good agreement, since the image fields are of lesser importance and the saddle point and the branch point never quite coalesce.

To see why UAA changes GOA drastically, we first note from equations (9b) and (9c) that $G(S_b)$ and $G(0)$ are of $O(R_m^{-1/2})$ when $R_m \to \infty$. When the observation angle approaches the critical angle, i.e., $S_b \to 0$, we use the small-argument approximation to the parabolic cylinder function in equation (9a) and find that

$$T_m^0 \sim e^{ik_1 R_m} \pi \left[ \frac{G(0) e^{-i(\pi/4)}}{R_m^{3/4} \Gamma(1/4)} + \frac{G'(0) e^{-i(3\pi/4)}}{R_m^{5/4} \Gamma(-1/4)} \right], \alpha_m = \theta_c \tag{11}$$

which is of $O(R_m^{-5/4})$. Thus $T_m^0$ is an important correction to $T_m^e$ when $\alpha_m \simeq \theta_c$. In GOA, $T_m^0$ is neglected when $\alpha_m \simeq \theta_c$.

When $\alpha_m < \theta_c$ and $R_m \to \infty$, we use the large-argument expansion to parabolic cylinder function (Whittaker and Watson, 1958)

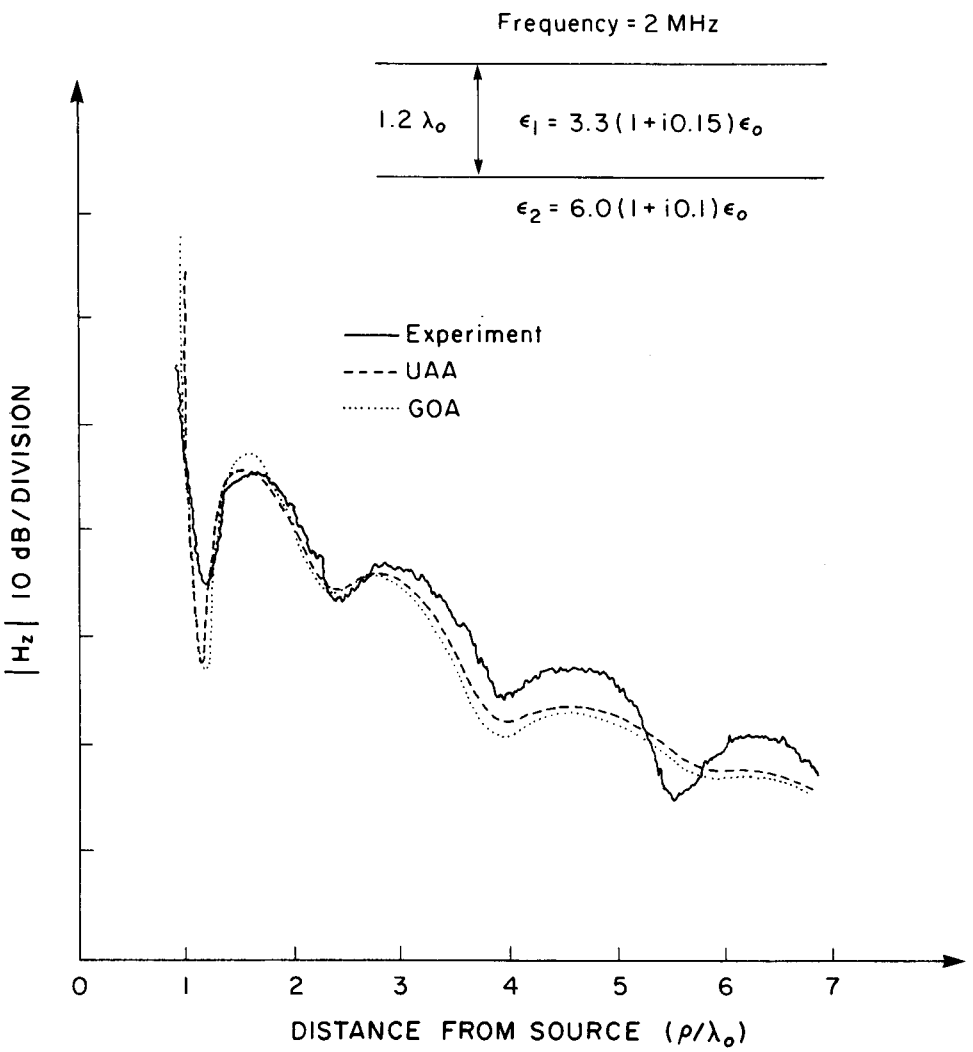


FIG. 4. Comparison of $H_z$ component with experimental data gathered from the Athabasca glacier using UAA and GOA.

in equation (9a) and obtain

$$T_m^0 \sim \frac{2\,e^{ik_1R_m}}{iR_m}(k^2 - k_1^2\sin^2\alpha_m)^{1/2}A_{m0}(k_1\sin\alpha_m). \quad (12)$$

As such, adding the above to the even part in equation (10), we obtain

$$T_m \sim \frac{2\,e^{ik_1R_m}}{iR_m}A_m(k_1\sin\alpha_m), \quad (13)$$

which is equal to that obtained by the ordinary saddle-point method in equation (4).

When $\alpha_m > \theta_c$ and $R_m \to \infty$, the arguments of parabolic cylinder functions in equation (8) change sign. Asymptotic expansion of the parabolic cylinder function exhibits Stoke's phenomenon (Whittaker and Watson, 1958), and we find that

$$T_m^0 \sim \frac{2\,e^{ik_1R_m}}{iR_m}(k^2 - k_1^2\sin^2\alpha_m)^{1/2}A_{m0}(k_1\sin\alpha_m) - \frac{2\exp[ik_1R_m\cos(\alpha_m - \theta_c)]\cos^{1/2}(\theta_c)}{R_m^2\sin^{3/2}(\alpha_m - \theta_c)\sin^{1/2}(\alpha_m)}A_{m0}(k)\sin\theta_c. \quad (14)$$

Combining equations (14) and (10), we obtain

$$T_m \sim \frac{2}{i}\frac{e^{ik_1R_m}}{R_m}A_m(k_1\sin\alpha_m) - \frac{2\exp[ik_1R_m\cos(\alpha_m - \theta_c)]\cos^{1/2}(\theta_c)}{R_m^2\sin^{3/2}(\alpha_m - \theta_c)\sin^{1/2}\alpha_m}A_{m0}(k)\sin\theta_c. \quad (15)$$

The first term is similar to the direct wave from the image source obtained by saddle-point approximation and the second term is similar to the lateral wave contribution (Brekhovskikh, 1960). This second term can also be obtained by evaluating the branch-point contribution using the steepest descent method. We note that the second term in equation (15), which is of higher order, is singular when $\alpha_m = \bar{\theta}_c$, i.e., when the observation point is at the caustics of geometrical optics. If the higher order approximation to equation (3) is obtained using the saddle-point method, the result also becomes singular at the caustics.

Consequently, we note the following: (1) The leading order saddle-point approximation to the image source term is equivalent to geometrical optics in diffraction theory; (2) the higher order approximation to the saddle-point method yields terms which are singular at the caustics, analogous to the geometrical theory of diffraction (Keller, 1962); and (3) the UAA, which is uniformly valid for all angle of observations, is analogous to the uniform asymptotic theory of diffraction (Lewis and Boersma, 1969). The uniform asymptotic theory removes singularities of the field at the caustics found in the geometrical theory of diffraction.

In conclusion, we see that GOA for the image source fields in the dipole interference field is valid if $R_m \to \infty$ and the angle of observation $\alpha_m$ is not close to $\theta_c$. When $\alpha_m \to \theta_c$, anomalous behavior of the field can be accounted for by the properties of parabolic cylinder functions in the UAA. As such, by using the UAA, we extend the range for which the approximation of the image source representation is valid to complement the normal mode expansion method which is efficient for thin layers only. Uniform asymptotic approximation to the field in the caustics for a source on top of a half-space has been obtained by Brekhovskikh (1960), using an informal approach. However, for the image-source field, it is necessary to separate the integrand into a branch-point free part, which can be approximated with spherical waves, and a part which needs to be approximated with parabolic cylinder functions.

## ACKNOWLEDGMENTS

This work was supported by NSF grant ENG78-23145 and Joint Services Electronics Program under contract no. DAAG-29-78-C-0020.

## REFERENCES

Annan, A. P., 1973, Radio interferometry depth sounding, part I: Theoretical discussion: Geophysics, v. 38, p. 557–580.
Annan, A. P., Waller, W. M., Strangway, D. W., Rossiter, J. R., Redman, J. D., and Watts, R. D., 1975, The electromagnetic response of a low-loss, two-layer, dielectric earth for horizontal electric dipole excitation: Geophysics, v. 40, p. 285–298.
Bleistein, N., and Handelsman, R. A., 1975, Asymptotic expansion of integrals: New York, Holt, Rinehart and Winston.
Brekhovskikh, L. A., 1960, Waves in layered media: New York, Academic Press.
Felsen, L. B., and Marcuvitz, N., 1973, Radiation and scattering of waves: New Jersey, Prentice-Hall.
Keller, J. B., 1962, Geometrical theory of diffraction: J. Opt. Soc. Am., v. 52, p. 116–130.
Kong, J. A., 1972, Electromagnetic fields due to dipole antennas over stratified anisotropic media: Geophysics, v. 38, p. 985–996.
——— 1975, Theory of electromagnetic waves: New York, Wiley-Interscience.
Kong, J. A., Shen, L. C., and Tsang, L., 1977, Field of an antenna submerged in dissipative dielectric medium: IEEE Trans. on Ant. and Prop., p. 887–889.
Kong, J. A., Tsang, L., and Simmons, G., 1974, Geophysical subsurface probing with radio-frequency interferometry: IEEE Trans. on Ant. and Prop., AP-22m p. 616–620.
Lewis, R. M., and Boersma, J., 1969, Uniform asymptotic theory of edge diffraction: J. Math. Phys., v. 10, p. 2291–2305.
Rossiter, J. R., LaTorraca, G. A., Annan, A. P., Strangway, D. W., and Simmons, G., 1973, Radio interferometry depth sounding, part II: Experimental results: Geophysics, v. 38, p. 581–599.
Rossiter, J. R., Strangway, D. W., Annan, A. P., Watts, R. D., and Redman, J. D., 1975, Detection of thin layers by radio interferometry: Geophysics, v. 40, p. 299–308.
Salvage, J. C., and Paterson, W. S. B., 1963, Borehole measurements in the Athabasca glacier: J. Geophys. Res., v. 68, p. 4521–4536.
Tsang, L., Brown, R., Kong, J. A., and Simmons, G., 1974, Numerical evaluation of electromagnetic field due to dipole antennas in the presence of stratified media: J. Geophys. Res., v. 79, p. 2077–2081.
Tsang, L., and Kong, J. A., 1973, Interference patterns of a horizontal electric dipole over layered dielectric media: J. Geophys. Res., v. 78, p. 3287–3300.
Wait, J. R., 1951, The magnetic dipole over the horizontal stratified earth: Can. J. Phys., v. 29, p. 577–592.
——— 1970, Electromagnetic waves in stratified media: New York, Pergamon Press.
———, Ed., 1971, Electromagnetic probing in geophysics: Boulder, Golem Press.
Whittaker, E. T., and Watson, G. N., 1958, A course in modern analysis: New York, Cambridge Univ. Press.

## APPENDIX

## UNIFORM ASYMPTOTIC EXPANSION OF AN INTEGRAL

An integral with an algebraic singularity at $t = t_b$ in the neighborhood of a saddle point at $t = 0$ can be expressed as

$$I = \int_C (t - t_b)^r g(t) e^{-\lambda f(t)} dt, \quad (A-1)$$

where $r$ can be fractional as well as negative integers, $\lambda$ is a large parameter, and $C$ is the integration path extending to infinity. The parameter $t_b$ measures the distance of singularity from the saddle point at $t = 0$. With the transformation

$$f(t) = f(0) + s^2, \quad (A-2)$$

we find

$$I = e^{-\lambda f(0)} \int_{C'} (s - s_b)^r G(s) e^{-\lambda s^2} ds, \quad (A-3a)$$

where

$$s_b = \sqrt{f(t_b) - f(0)}, \tag{A-3b}$$

$$G(s) = \left(\frac{t - t_b}{s - s_b}\right)^r g(t)\,\frac{dt}{ds}, \tag{A-3c}$$

and $C'$ is the image of $C$ on the $s$-plane under the transformation (A-2).

A leading order approximation to equation (A-3) can be obtained by approximating $G(s)$ with a polynomial that interpolates the branch point and the saddle point, i.e., letting

$$G(s) = \gamma_0 + \gamma_1(s - s_b) + s(s - s_b)G_1(s), \tag{A-4}$$

where $\gamma_0 = G(s_b)$ and $\gamma_1 = [G(s_b) - G(0)]/s_b$. It can be shown that the third term in equation (A-4) contributes to a term of $O(1/\lambda)$ smaller than the first two terms. Consequently, we find

$$I \sim e^{-\lambda f(0)} \int_{C'} ds(s - s_b)^r[\gamma_0 + \gamma_1(s - s_b)]e^{-\lambda s^2}. \tag{A-5}$$

With the change of variable to $u = \sqrt{2\lambda}(s - s_b)$, we obtain

$$I \sim e^{-\lambda[f(0)+s_b^2]} \int_{-\infty}^{\infty} du \left[\frac{\gamma_0 u^r}{(2\lambda)^{(r+1)/2}} + \frac{\gamma_1 u^{r+1}}{(2\lambda)^{(r+2)/2}}\right] \cdot \exp - \left(\frac{u^2}{2} + \sqrt{2\lambda}\, s_b u\right). \tag{A-6}$$

Notice that the original path of integration has been deformed to the real axis. The real axis integration is taken above the singularity at the origin if the original path of integration is above the singularity and, conversely, if the original path of integration is below the origin. Equation (A-6) can be integrated exactly, giving

$$I \sim e^{-\lambda[f(0)+s_b^2]}\left[\frac{\gamma_0}{(2\lambda)^{(r+1)/2}}\, W_r(\sqrt{2\lambda}\, s_b) + \frac{\gamma_1}{(2\lambda)^{(r+2)/2}} \cdot W_{r+1}(\sqrt{2\lambda}\, s_b)\right] \tag{A-7}$$

where

$$W_k(\sqrt{2\lambda}\, s_b) = \begin{cases} \sqrt{2\pi}\, e^{(\pi/2)ki} e^{\lambda(s_b^2/2)} D_k(i\sqrt{2\lambda}\, s_b) & \begin{pmatrix}\text{integration path}\\ \text{above origin}\end{pmatrix} \\ \sqrt{2\pi}\, e^{-(\pi/2)ki} e^{\lambda(s_b^2/2)} D_k(-i\sqrt{2\lambda}\, s_b) & \begin{pmatrix}\text{integration path}\\ \text{below origin}\end{pmatrix}. \end{cases} \tag{A-8}$$